Characterizing Shales as Seals for CO_2 Containment and Shales as Reservoirs for Geologic Storage of CO_2

Dustin Crandall[1], Angela L. Goodman[1], Barbara Kutchko[1], Sean Sanguinito[1,2], Johnathan Moore[1,2], Magdalena Gill[1,2], Guanyi Lu[3], Patricia Cvetic[1,2], Mary Tkach[3], Sittichai Natesakhawat[1,4]

[1]US Department of Energy, National Energy Technology Laboratory, Pittsburgh, PA /Morgantown, WV; [2]LRST, Pittsburgh, PA; [3]Oak Ridge Institute for Science and Education, Oak Ridge, TN; [4]University of Pittsburgh, Pittsburgh, PA.

Research & Innovation Center

NATIONAL ENERGY TECHNOLOGY LABORATORY

Abstract

When storing CO_2 in the subsurface, shale formations are expected to be used as sealing layers because of their low permeability. Due to its buoyant nature, injected CO_2 will gradually rise towards the surface until it is trapped by an impermeable shale formation. The CO_2 will react with the shale and components of shale (i.e. organic matter, kerogen, minerals, clays) altering the shale petrophysical properties and potentially impacting the shale formation's ability to trap CO_2 in the subsurface. It is vital to investigate the types of reactions that will occur at this CO_2-shale interface and increase our understanding of the role these interactions play in maintaining CO_2 permeance in the subsurface. Several techniques used to analyze CO_2-shale interactions include feature relocation scanning electron microscopy (SEM), surface area and pore size analysis, and in-situ Fourier Transform Infrared (FTIR) spectroscopy. Results indicate that porosity is significantly increased in carbonate rich shales while silicate rich shales experience an increase in microfractures. Changes in various pore sizes are also observed with the abundance of nano sized pores typically decreasing after CO_2-fluid reactions while micro-pores increase. As CO_2 interacts with shale and the shale sealing properties are potentially altered, it is important to investigate and quantify stress related changes (i.e. microfracturing). To examine stress related changes in shale, three-point bending experiments are conducted on shale beams using AE (acoustic emission) monitoring. The impact of bedding orientation on AE was examined and found that more AE events have been recorded for cases where loading is applied transverse as opposed to parallel to bedding.

Eau Claire (Shale Seal)

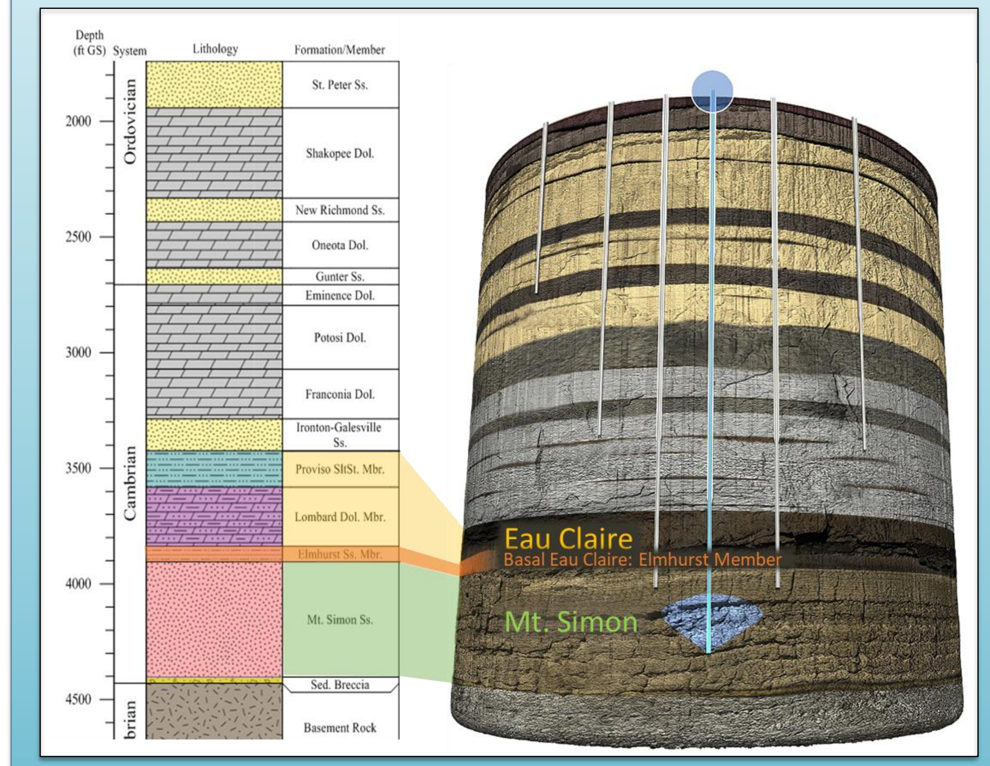

Image by www.cranedigital.com for FutureGen Alliance

FutureGen 2.0 Project

- Target reservoir: Mt. Simon Sandstone
- Sealing formation: Eau Claire Formation
- Our study target: Basal Eau Claire: Elmhurst Member
- Interbedded sandstone, siltstone, and shale

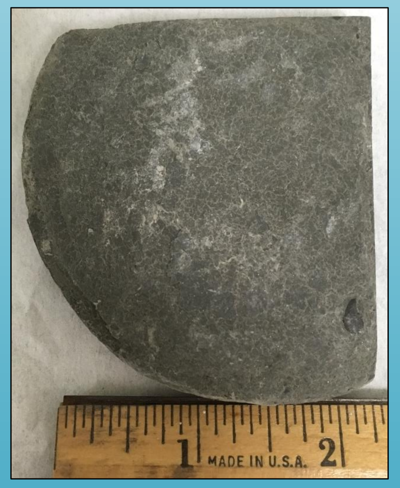

Top: Stratigraphic column of the FutureGen site showing the Mt. Simon Sandstone (CO_2 storage reservoir) and Eau Claire Formation (CO_2 sealing formation). Right: Eau Claire core.

Shear Behavior

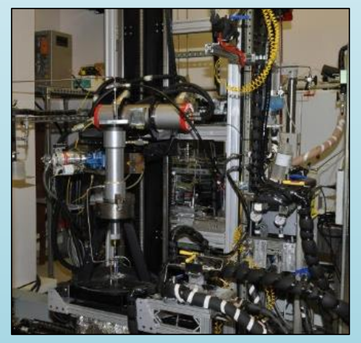

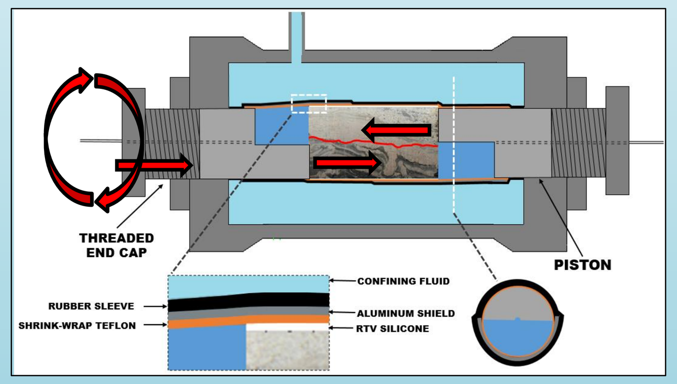

Top Left: North Star Imaging M5000 Industrial CT Scanner.
Top Right: Modified core holder for fracture experiments on Eau Claire.

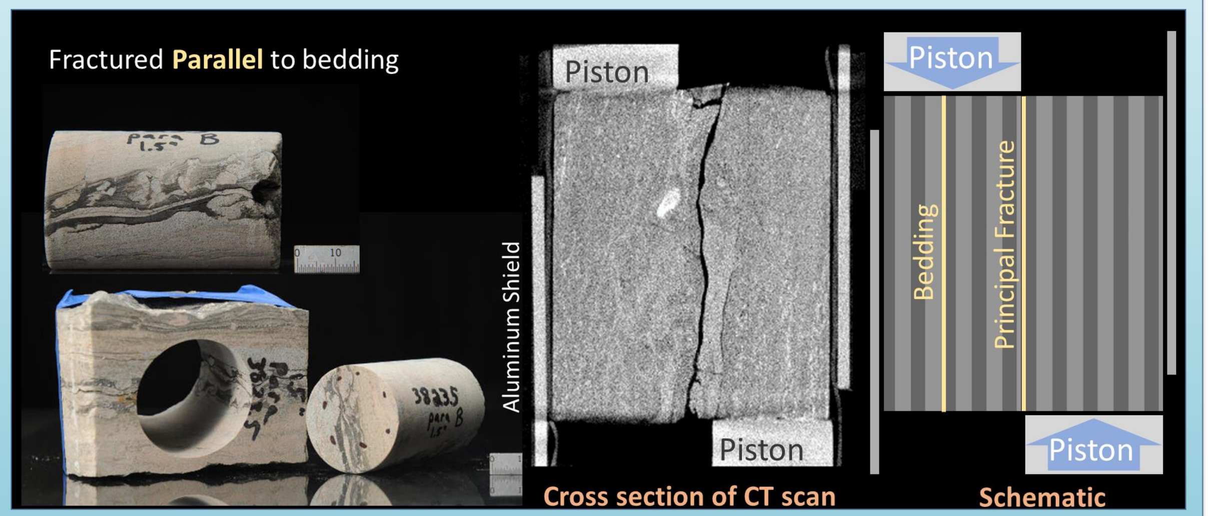

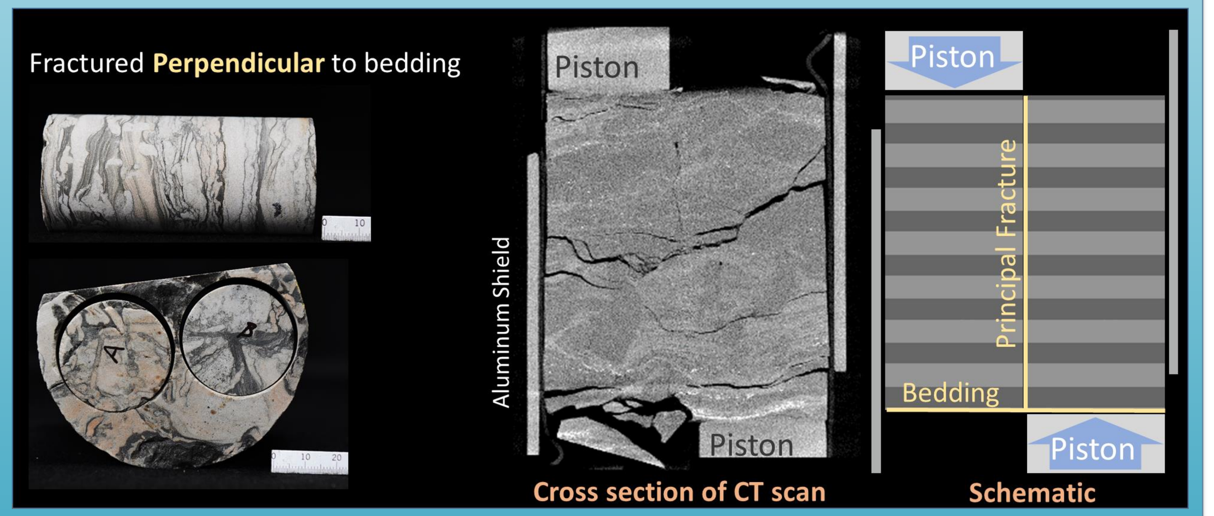

Fracturing (mainly sheared parallel to bedding)

- Bedding planes and shale layers are zones of weakness
- Secondary fracture formation common
- Fracturing along shale interbeds common

Fracture dilation

- Common but not uniform

Gouge and Microfabric Influence

- Can limit *T* even given concurrent fracture dilation
- Biggest effects where shale layers parallel principal fracture
- Least effect where shear is perpendicular and shale a minor lithological constituent

Acoustic Emission

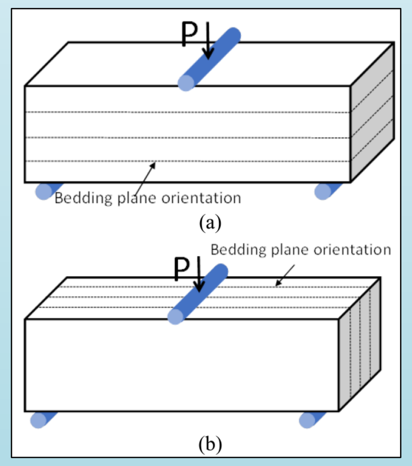

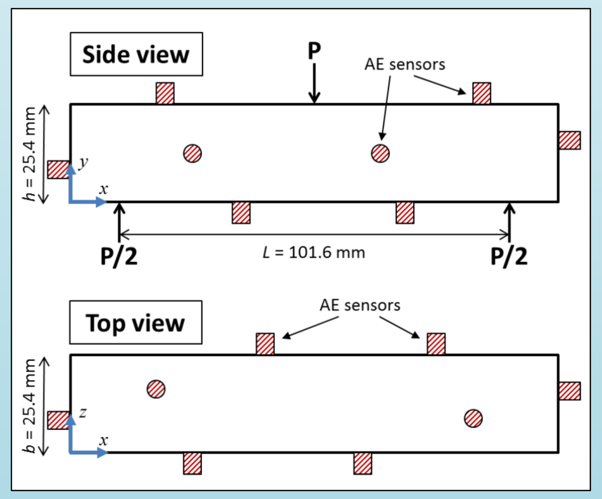

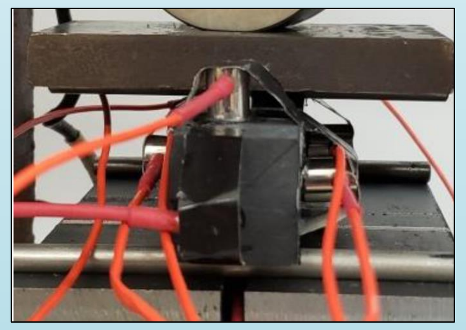

Left: Three-point loading configurations: (a) load applied perpendicular to bedding; (b) load applied parallel to bedding. Middle: Sensor layout on the sample. Right: Side view from end of sample (Marcellus Shale) being tested. (Lu et al., 2019).

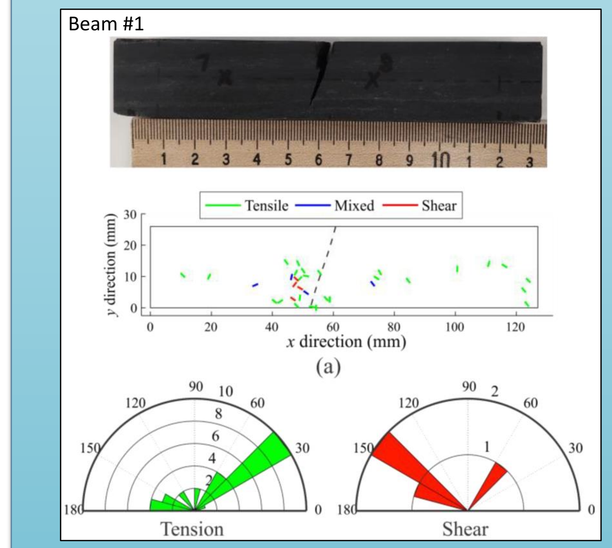

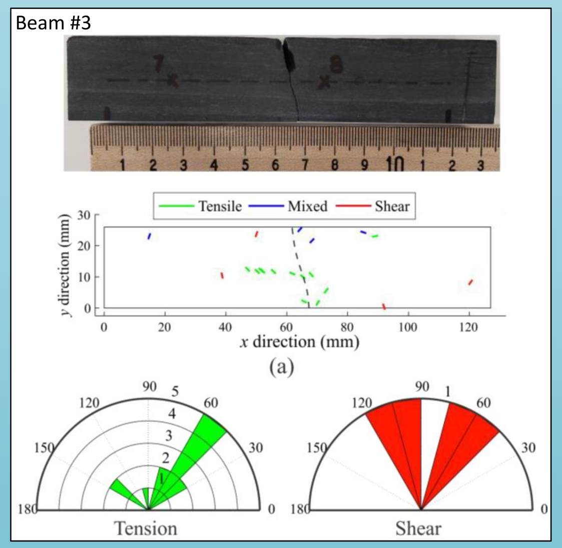

Beam #	Loading Direction	Maximum tensile stress (MPa)
1	Perpendicular	29
3	Perpendicular	32.6
2	Parallel	41.8
4	Parallel	36.7

Loading configurations for each Beam.

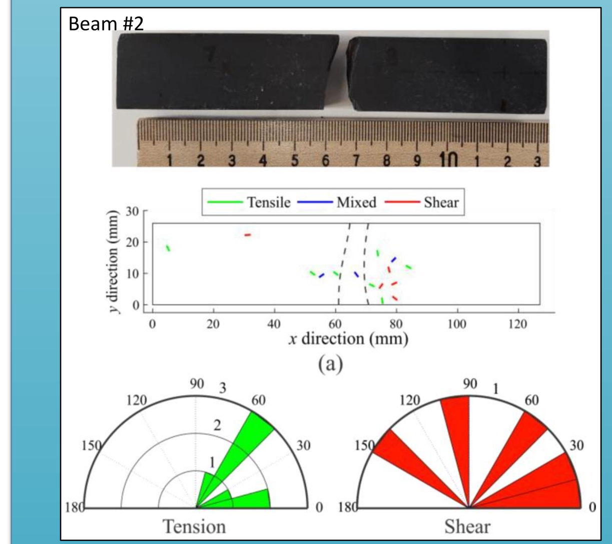

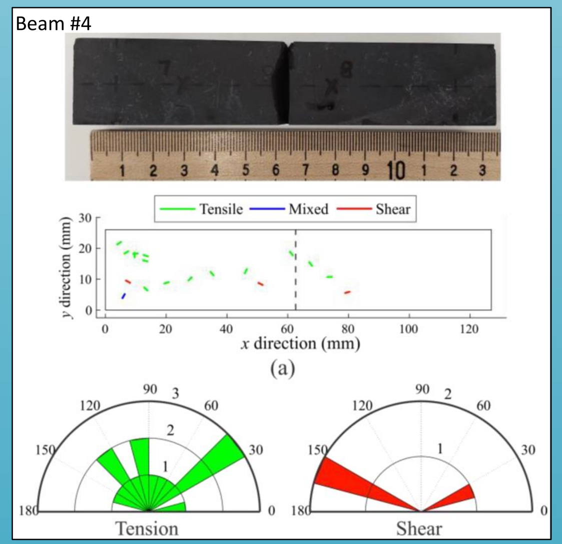

Detailed AE results for Beams #1-4 showing (top) photograph of failed sample and locations/classifications of the micro cracks detected by AE monitoring; (bottom) Crack motion for tensile (left) and shear (right) cracks. Results are plotted in the angle with respect to the x-axis. (Lu et al., 2019).

Amherstberg (Non-shale Seal)

Michigan Basin Phase II Project

- Target reservoir: Bass Islands Group
- Sealing formation: Amherstberg Formation
- Our study target: Amherstberg: Meldrum Member
- Carbonate, microcrystalline wackstone

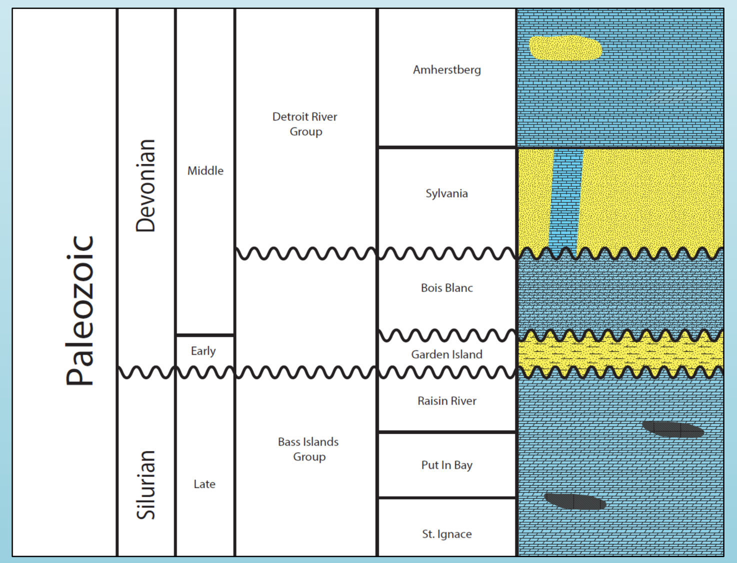

Reagent	Wt (g) added
CaCl2·2H2O	265.57
MgCl2·6H2O	86.97
NaCl	54.18
KCl	17.67
SrCl2·6H2O	7.12
NaBr	3.94
NaHCO3	0.45
Na2SO4	0.003

Left: Brine recipe used for reactions. Based off the Sylvania sandstone (underlying the Amherstberg) (Wilson and Long, 1992). Right: Amherstberg sample from St. Charlton Well #4-30, depth of 3037.5 feet.

Relevant References

- Dieterich, M., Kutchko, B., Goodman, A., 2016. Characterization of Marcellus Shale and Huntersville Chert before and after exposure to hydraulic fracturing fluid via feature relocation using field-emission scanning electron microscopy. Fuel, p. 227-235.
- Gardner, Weston Clive, 1974, Middle Devonian Stratigraphy and Depositional Environments in the Michigan Basin: Michigan Basin Geological Society, Special Papers
- Harrison, W. B., G. M. Grammer, and D. A. Barnes, 2009, Reservoir characteristics of the Bass Islands dolomite in Otsego County, Michigan: Results for a Saline Reservoir, CO2 Sequestration Demonstration: Environmental Geosciences, v. 16, no. 3, p. 139–151, doi:10.1306/eg.05080909011.
- Kutchko, B.G., Goodman, A.L., Rosenbaum, E., Natesakhawat, S., Wagner, K., 2013. Characterization of coal before and after supercritical CO2 exposure via feature relocation using field-emission scanning electron microscopy. Fuel, v. 107, p. 777-786.
- Lu, G., Crandall, D., Bunger, A.P., 2019. Impact of bedding orientation on acoustic emission generated by shale subjected to bending, American Rock Mechanics Association, v.19-1786, p. 7.
- Sanguinito, S., Goodman, A., Tkach, M., Barbara, K., Culp, J., Natesakhawat, S., Fazio, J., Fukai, I., Crandall, D., 2018, Quantifying dry supercritical CO2-induced changes of the Utica Shale: Fuel, v. 226, p. 54-64.
- US-DOE-NETL, 2015. Carbon Storage Atlas, fifth edition. U.S. Department of Energy—National Energy Technology Laboratory—Office of Fossil Energy.
- USGS, 2008, Carbon Sequestration to Mitigate Climate Change: USGS Bulletin, p. 1-4.
- USGS, Department of the Interior, 2013, National Assessment of Geologic Carbon Dioxide Storage Resources—Methodology Implementation: Open File Report 2013-1055, p. 1-35.
- Wilson, T.P. and Long, D.T., 1993. Geochemistry and isotope chemistry of Michigan Basin brines: Devonian formations. Applied Geochemistry, v. 8, no. 1, p. 81-100.

Scanning Electron Microscopy

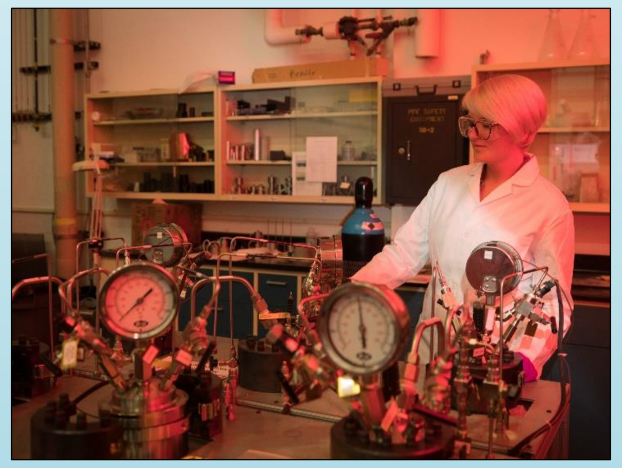

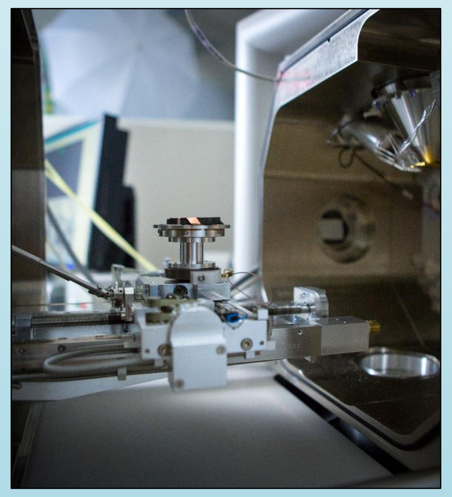

Left: Scanning Electron Microscope (SEM). Middle: High pressure reaction vessels. Right: SEM stage with sample.

SEM/EDS images of Amherstberg limestone. A) Unreacted sample displaying calcite (light gray matrix), and Mg-rich dolomite (dark gray matrix). (B) Dry-CO_2 reacted limestone shows surface pitting and pore spaces as circled. C) Elemental map before dry CO_2 exposure. D) Elemental map after dry CO_2 exposure.

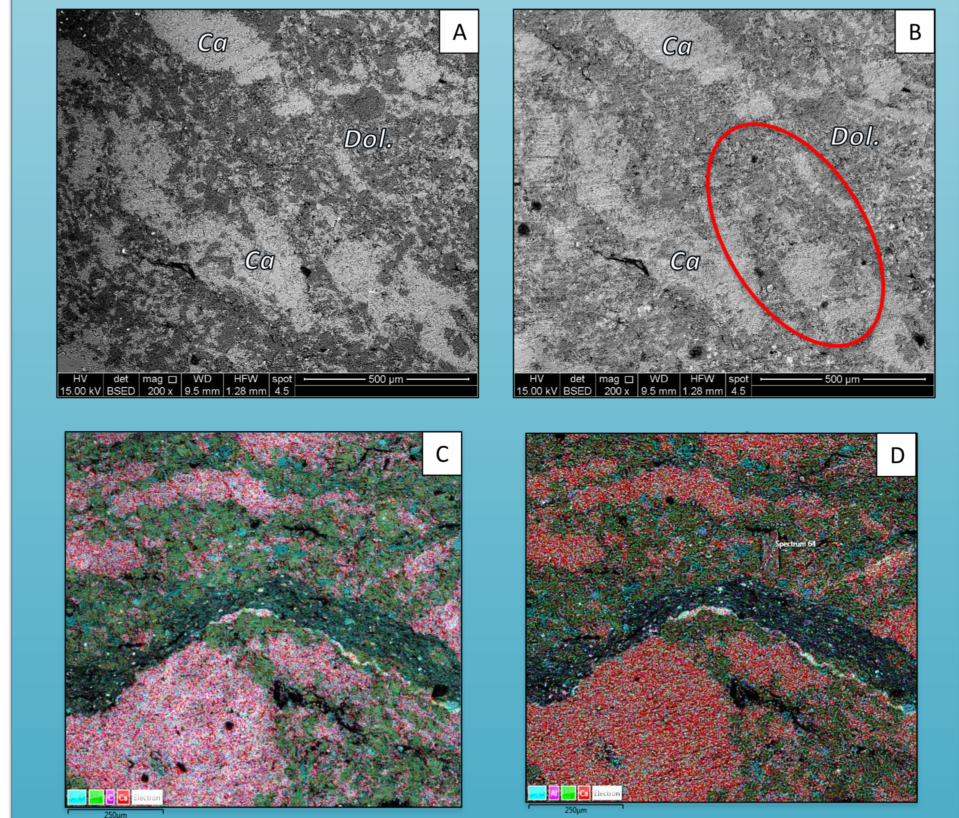

SEM/EDS images of Amherstberg limestone. A) Unreacted sample displaying calcite (light gray matrix), dolomite (dark gray matrix), shale interbed (outlined in red), and pyrite (white). B) Brine-CO_2 reacted limestone featuring euhedral NaCl crystals and bands of various salt crystals, including $CaCl_2$, $MgCl_2$, and KCl, covering and forming within the sample surface; Calcium-rich species are no longer present in the image. C) Elemental map before brine-CO_2 exposure. D) Elemental map after brine-CO_2 exposure.

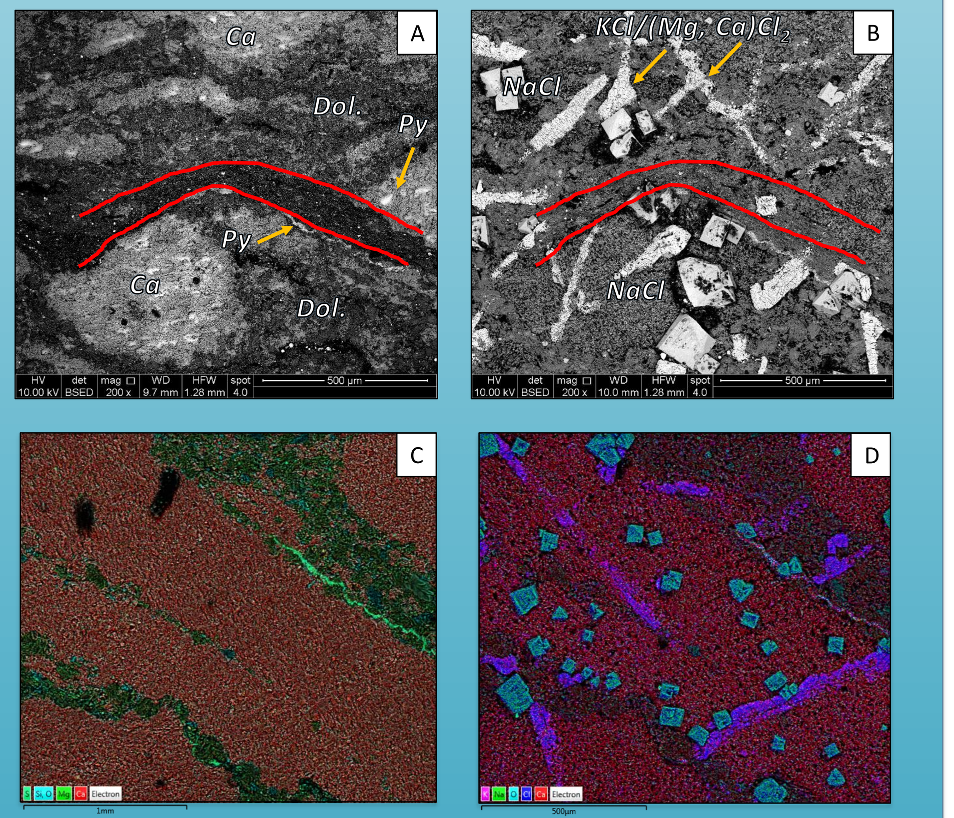

U.S. DEPARTMENT OF ENERGY

Science & Engineering To Power Our Future

This technical effort was performed in support of the National Energy Technology Laboratory's ongoing research under the RES contract DE-FE0004000